Hindawi
International Journal of Antennas and Propagation
Volume 2023, Article ID 5557062, 15 pages
https://doi.org/10.1155/2023/5557062

Research Article

Decoupling Network for Closely Spaced Tx/Rx Antennas Using a Directional Coupler and Transmission Lines

Jeong-Hun Park, Jeong-Eun Roh, and Moon-Que Lee

School of Electrical and Computer Engineering, University of Seoul, Siripdae-gil 163, Dongdaemun-gu, Seoul 130-743, Republic of Korea

Correspondence should be addressed to Moon-Que Lee; mqlee@uos.ac.kr

Received 2 February 2023; Revised 2 April 2023; Accepted 4 April 2023; Published 24 April 2023

Academic Editor: Hervé Aubert

This paper presents an efficient decoupling network using a single directional coupler and transmission lines for closely spaced Tx/Rx antennas in single polarized radar applications. The isolation between both antennas can be enhanced by controlling the phase of the Tx leakage signal and the coupling coefficient of the directional coupler. Its structure provides no loss of Tx/Rx paths excepting minute loss due to the coupling of the directional coupler. The Tx leakage is more insensitive to the antenna impedance variation compared with a conventional monostatic system. The design process is as follows: First, closely separated Tx/Rx antennas were designed and their isolation ($\mathbf{I}_a$) was extracted. Second, the directional coupler was designed with its coupling coefficient = $|\mathbf{I}_a|$. Finally, both were connected by transmission lines, of which phases were adjusted for the coupled and antenna-isolated signals with 180° phase difference. The Tx/Rx antennas without and with the decoupling network have 15-dB bandwidths of 23.98–24.43/23.98–24.50 GHz and 23.80–24.36/23.80–24.45 GHz, respectively. Gains of 8.17/8.39 and 8.72/8.73 dBi and efficiencies of 60.56%/60.77% and 63.0%/61.8% in the Tx/Rx antennas without and with the decoupling network were achieved at 24.1 GHz, respectively. The dimension of the proposed antenna is $1.62\lambda_0 \times 2.09\lambda_0 \times 0.0204\lambda_0$. The K-band antennas show a good Tx-Rx isolation of 29.3–67.9 dB which was superior at least 9 dB to the conventional antennas.

1. Introduction

Short-range radars using microwave technology have been widely applied in various applications such as speed/motion detection, automotive sensors, healthcare monitoring, and collision avoidance [1–5]. Frequency modulated continuous wave (FMCW) and Doppler radars are actively studied since continuous wave (CW) radars are beneficial to compactness and cost-effectiveness [5]. In receivers with asymmetric structure using an unbalanced LO signal, the LO self-mixing results in relatively large DC offsets in a baseband. In radar transceivers, since the output of an oscillator shares the LO and the Tx signals, the LO leakage signal causing the LO self-mixing can be represented as the Tx leakage signal. Also, since the frequencies of Tx and Rx signals are generally or occasionally close, the frequency of the baseband is close to DC. The DC offsets due to the Tx leakage signal is an interference signal to the desired signal and degrades the radar receiver sensitivity. To enhance the radar receiver sensitivity, the Tx leakage signal should be mitigated. Because it is hard to use a duplexer for splitting Tx and Rx signals, which are close, the Tx-Rx isolation of the Tx/Rx antennas plays a key role in the radar receiver sensitivity.

Various radar transceiver architectures have been explored to improve Tx-Rx isolation. Compared with bistatic architecture, a monostatic system using a single Tx/Rx antenna has smaller circuit size but lower Tx-Rx isolation. To suppress the leakage signal from Tx to Rx in the monostatic system using a single antenna, an additional duplexing network such as a quadrature hybrid, circulator, or directional coupler is required. In the bistatic system using a single Tx/Rx antenna pair, sufficient spacing between Tx

and Rx antennas is required for the reduction of the Tx leakage. Figures 1(a) to 1(d) show, respectively, the four conventional approaches to reduce the Tx leakage signal [5].

Methods with the quadrature hybrid uses power split port and isolation port for antenna feed and leakage suppression, respectively. Techniques with the circulator make use of its directionality of the power flow. Schemes with the directional coupler uses the through port, coupled port, and isolation port for antenna feed, signal receive, and leakage suppression. The directional coupler or hybrid coupler undergoes the loss of the wanted signal by 3 dB power splits in the Tx and Rx paths or coupling in the Rx path, respectively. Moreover, in aforementioned schemes for the monostatic systems, the receiver remains exposed to a significant Tx leakage signal due to the reflection from antenna on the Tx path and the intrinsic isolation performance of components such as quadrature hybrids, circulators, and directional couplers [5]. Commercially available hybrid couplers, directional couplers, or circulators typically provide the isolation of approximately 25 dB when well-matched [5]. In monostatic systems with the antenna that is not well-matched, the Tx leakage increases, which adversely affects the receiver sensitivity. Various monostatic systems using a single antenna have been studied for the reduction of Tx leakage: balanced topologies [6, 7], quadrature topologies [8, 9], and configurations using a directional coupler [10–12]. Methods to reduce the Tx leakage considering antenna impedance variation have been introduced in references [10, 11].

Bistatic architecture shown in Figure 1(d) is not suitable for compact radar module since both antennas should be separated from each other for sufficient isolation. Various other approaches for high Tx-Rx antenna isolation have been introduced for Tx/Rx antenna pair geometry [13]: decoupling networks [14–17], parasitic elements [18, 19], defected ground structures [20, 21], and neutralization lines [22, 23]. Among them, schemes using the decoupling network for Tx leakage cancelation have been proposed, of which decoupling networks are two directional couplers, strip monopole, and suspended transmission line shorted to the ground plane with capacitor [14–17].

In this work, Tx/Rx antennas with horizontal polarizations for K-band automotive radar sensors, which have been widely used in advanced driver assistance [24], have been investigated. Power losses in the Tx and Rx paths degrade the power level of the wanted signal. Poor Tx-Rx isolation increases the interference of the DC offset. The bistatic architecture, which has no power losses in the Tx and Rx paths and sufficiently high Tx-Rx isolation, is suitable for higher receiver sensitivity. The neutralization-line technique is useful for simple geometry and compactness. The neutralization-line technique cannot be realized on the microwave substrate, since the characteristic impedance of 216 Ω corresponds to the microstrip line width of 1 μm on the microwave substrate RO4350B with a thickness of 10 mil and a relative dielectric constant ε_r of 3.48 as well as the required characteristic impedance of the neutralization line is 500 Ω for the designed Tx and Rx antennas operating in the frequency range of 24 to 24.25 GHz allocated for the K-band radar operation. In this paper, authors propose a new compact approach, a simple and efficient decoupling network adopting a sole directional coupler for closely spaced Tx/Rx antennas in single polarized automotive sensors with transmission and reception of horizontally polarized electric fields. The horizontal polarization is adopted for automotive radar target detection since the horizontally polarized backscattering coefficients are smaller than the vertically polarized backscattering coefficients for dry and wet asphalts at large incidence angels of 25° to 80° at 24 GHz [25]. The proposed decoupling network is a simple structure, occupies small circuit size, and has easy implementation, which is realized by adjusting the phase of the Tx leakage signal and the coupling coefficient of the directional coupler. The operation of the decoupling network adopting the directional coupler is explained using the S-parameters of the directional coupler and Tx/Rx antennas. The effect of the antenna impedance on the Tx leakage is analyzed. The suppressed Tx leakage is more insensitive to the antenna impedance variation compared with the conventional monostatic system using the quadrature hybrid, circulator, or directional coupler.

2. Proposed Decoupling Network Design

2.1. Theory. The schematic of Tx/Rx antennas with the directional coupler is shown in Figure 2. The Tx signal is induced at port 1 and the signal leaks to the Rx path at port 4.

The Tx-Rx isolation, the power ratio of the Tx leakage signal to the Tx input signal can be expressed in terms of the scattering parameters. The S-parameter matrices of the directional coupler and Tx/Rx antennas are as follows:

$$[s]_{\text{coupler}} = \begin{bmatrix} 0 & T & I & C \\ T & 0 & C & I \\ I & C & 0 & T \\ C & I & T & 0 \end{bmatrix}, \tag{1}$$

$$[s]_{\text{antennas}} = \begin{bmatrix} \Gamma_{Txa} & I_a \\ I_a & \Gamma_{Rxa} \end{bmatrix}. \tag{2}$$

The through, coupling, and isolation of the coupler are denoted as T, C, and I, respectively. For simplicity, the perfect matched conditions and symmetric and reciprocal properties are applied in equation (1). The reflection coefficients of Tx and Rx antennas and coupling between two antennas are denoted as Γ_{Txa}, Γ_{Rxa}, and I_a in equation (2), respectively. When the coupler is connected to antennas at ports 2 and 3 as shown in Figure 2, the reflected waves at ports 1, 2, 3, and 4, b_1, b_2, b_3, and b_4, are represented in terms of S-parameters of the coupler and antennas, and the incident waves at ports 1, 2, 3, and 4, a_1, a_2, a_3, and a_4, are as follows:

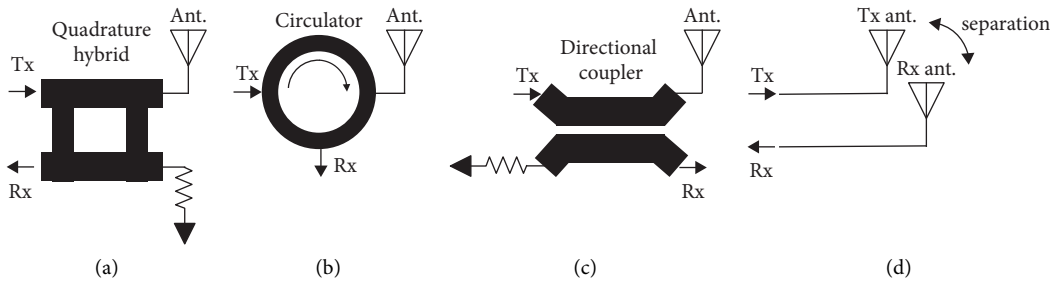

Figure 1: Conventional methods to isolate Tx and Rx using (a) a quadrature hybrid, (b) a circulator, (c) a directional coupler in monostatic system, and (d) antenna space separation.

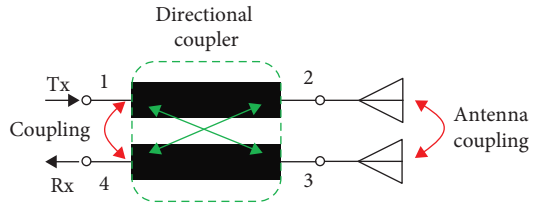

Figure 2: Schematic of Tx/Rx antennas with single directional coupler.

$$\begin{bmatrix} b_1 \\ b_2 \\ b_3 \\ b_4 \end{bmatrix} = \begin{bmatrix} 0 & T & I & C \\ T & 0 & C & I \\ I & C & 0 & T \\ C & I & T & 0 \end{bmatrix} \begin{bmatrix} a_1 \\ a_2 \\ a_3 \\ a_4 \end{bmatrix}, \tag{3}$$

$$\begin{bmatrix} b_2 \\ b_3 \end{bmatrix} = \begin{bmatrix} \Gamma_{Txa} & I_a \\ I_a & \Gamma_{Rxa} \end{bmatrix} \begin{bmatrix} a_2 \\ a_3 \end{bmatrix}. \tag{4}$$

Substituting equation (4) into equation (3), the reflected waves, b_1 and b_4, can be expressed by the incident waves, a_1 and a_4 as follows:

$$b_1 = \frac{1}{1 - I_a C - \Gamma_{Txa}\Gamma_{Rxa}C^2/(1 - I_a C)} \left\{ \Gamma_{Txa}T^2 + \Gamma_{Rxa}I^2 + 2I_a TI + \frac{I_a\left(\Gamma_{Txa}T^2 + \Gamma_{Rxa}I^2\right) + 2\Gamma_{Txa}\Gamma_{Rxa}TI}{1 - I_a C} \bullet C \right\}$$

$$\bullet a_1 + \left[C + \frac{1}{1 - I_a C - \Gamma_{Txa}\Gamma_{Rxa}C^2/(1 - I_a C)} \left\{ I_a\left(T^2 + I^2\right) + \left(\Gamma_{Txa} + \Gamma_{Rxa}\right)TI + \frac{\Gamma_{Txa}\Gamma_{Rxa}\left(T^2 + I^2\right) + \left(\Gamma_{Txa} + \Gamma_{Rxa}\right)I_a TI}{1 - I_a C} \bullet C \right\} \right] \bullet a_4, \tag{5}$$

$$b_4 = \left[C + \frac{1}{1 - I_a C - \Gamma_{Txa}\Gamma_{Rxa}C^2/(1 - I_a C)} \left\{ I_a\left(T^2 + I^2\right) + \left(\Gamma_{Txa} + \Gamma_{Rxa}\right)TI + \frac{\Gamma_{Txa}\Gamma_{Rxa}\left(T^2 + I^2\right) + \left(\Gamma_{Txa} + \Gamma_{Rxa}\right)I_a TI}{1 - I_a C} \bullet C \right\} \right]$$

$$\bullet a_1 + \frac{1}{1 - I_a C - \Gamma_{Txa}\Gamma_{Rxa}C^2/(1 - I_a C)} \left\{ \Gamma_{Rxa}T^2 + \Gamma_{Txa}I^2 + 2I_a TI + \frac{I_a\left(\Gamma_{Rxa}T^2 + \Gamma_{Txa}I^2\right) + 2\Gamma_{Txa}\Gamma_{Rxa}TI}{1 - I_a C} \bullet C \right\} \bullet a_4, \tag{6}$$

An equation related to Tx-Rx isolation can be derived from equation (6) as follows:

$$b_4 = \left[C + \frac{1}{1 - I_a C - \Gamma_{Txa}\Gamma_{Rxa}C^2/(1 - I_a C)} \left\{ I_a\left(T^2 + I^2\right) + \left(\Gamma_{Txa} + \Gamma_{Rxa}\right)TI + \frac{\Gamma_{Txa}\Gamma_{Rxa}\left(T^2 + I^2\right) + \left(\Gamma_{Txa} + \Gamma_{Rxa}\right)I_a TI}{1 - I_a C} \bullet C \right\}\right] \bullet a_1. \quad (7)$$

Next, three terms in equation (7) are assumed as follows:

$$1 - I_a C - \frac{\Gamma_{Txa}\Gamma_{Rxa}C^2}{1 - I_a C} \approx 1, \quad (8)$$

$$I_a I^2 \approx 0, \quad (9)$$

$$\frac{\Gamma_{Txa}\Gamma_{Rxa}\left(T^2 + I^2\right) + \left(\Gamma_{Txa} + \Gamma_{Rxa}\right)I_a TI}{1 - I_a C} \cdot C \approx 0. \quad (10)$$

A simplified equation related to the Tx-Rx isolation can be derived from equations (7)–(10) as follows:

$$b_4 \approx \left[C + \left\{I_a T^2 + \left(\Gamma_{Txa} + \Gamma_{Rxa}\right)TI\right\}\right] \cdot a_1. \quad (11)$$

To simplify equation (11), let $(\Gamma_{Txa} + \Gamma_{Rxa})TI$, which is, the Tx leakage related to the antenna impedance variations is 0, then C satisfying the cancelation of the Tx leakage is as follows:

$$C = \frac{1 - \sqrt{1 + 4{I_a}^2 T^2}}{2I_a} \approx T^2 I_a e^{j\pi}, \quad (12)$$

where C and T in the intrinsic directional coupler are expressed mathematically in the form of $|C|e^{j0}$ and $|T|e^{j(\pi/2)}$, respectively, considering both the phases. Here, the coupling of the directional coupler, C, has no value satisfying equation (12) except antenna coupling, I_a with phase of $2n\pi$. To make the phase of I_a be $2n\pi$, the directional coupler and antennas should be adjoined by additional two transmission lines with the characteristic impedance of 50 Ω and electrical length of θ_{TL}, as shown in Figure 3. Assuming $|T| \approx 1$, C for Tx-Rx leakage cancelation is expressed as follows:

$$C \approx \left|I_a\right| = \left|I_a\right|e^{j\left(2\theta_{TL} + \theta_{Ia}\right)}. \quad (13)$$

With $2\theta_{TL} + \theta_{Ia} = 2n\pi$, the isolation of the Tx and Rx antennas including the additional two transmission lines can be represented as follows:

$$\begin{aligned} I_{a,m} &= \left|I_a\right|e^{j\left(2\theta_{TL} + \theta_{Ia}\right)} \\ &= \left|I_a\right|. \end{aligned} \quad (14)$$

Then, the antenna isolation term, I_a in equations (7)–(10) can be substituted to $|I_a|$. The Tx leakage levels with the reflection coefficients of 15, 20, 25, and 30 dB against the phase of the delay line from equation (7) is depicted in Figure 4, assuming that the phase of the antenna coupling, θ_{Ia} is set to 360°. As expected by equation (13), each Tx leakage level is lowest for each return loss with the delay line phase of around 360°. Previously, equation (7) is simplified to equation (11), assuming equations (8)–(10). Figures 5(a) and 5(b) depict the Tx leakage levels against the antenna coupling and return loss of the Tx and Rx antennas with $I - C = 10$ dB from equations (7) and (11), respectively. Figures 6(a) and 6(b) show the Tx leakage levels with $I - C = 15$ dB from equations (7) and (11), respectively. From equations (7) and (11), both Tx leakage levels with $I - C = 10$ dB are better with higher return loss and antenna coupling, but the Tx leakage from equation (7) is more sensitive to the antenna coupling and insensitive to the return loss than the Tx leakage from equation (11). Both Tx leakage levels with $I - C = 15$ dB from equation (7) is also more insensitive to the return loss than the Tx leakage from equation (11). Especially, both Tx leakage levels from equations (7) and (11) with $I - C = 15$ dB have similar tendency for the return loss from 10 to 15 dB. The simplified equation (11) is acceptable providing the return loss from 10 to 15 dB and $I - C = 15$ dB. The simplified equation (11) with $I - C = 10$ dB is different from equation (7), but equation (11) with $I - C = 10$ dB is helpful in improving the Tx leakage level and simply presuming the Tx leakage level, given the return loss from 10 to 15 dB. In the practical case, the term $(\Gamma_{Txa} + \Gamma_{Rxa})TI$ in equation (11) in addition to the terms in equations (8)–(10) have an effect on the Tx leakage. The Tx leakages using equations (7) and (11) are compared varying the reflection coefficients of the Tx and Rx antennas. In comparison, the Tx-Rx isolations against the magnitude and phase of the reflection coefficients with $\Gamma_{Txa} = \Gamma_{Rxa}$ and the phase of the reflection coefficients with $|\Gamma_{Txa}| = |\Gamma_{Rxa}|$ are addressed for representing a 3-dimensional data of $(|\Gamma_a|, \angle\Gamma_a, I_{Tx-Rx})$ and $(\angle\Gamma_{Txa}, \angle\Gamma_{Rxa}, I_{Tx-Rx})$, respectively, even though, practically, both reflection coefficients are not identical to each other. Furthermore, considering the Tx/Rx antennas and directional coupler, which were designed and fabricated in this work, the directional coupler was set to have a coupling coefficient of 20 dB and isolation of 30 dB for Tx leakage suppression of the antenna, which has 20 dB isolation. The Tx leakage levels against the magnitudes and phases of the reflection coefficients of the Tx and Rx antennas from equations (7) and (11) are shown in Figures 7(a) and 7(b), respectively, assuming that the reflection coefficient of the Tx antenna is identical to that of the Rx antenna. Both the Tx leakage levels with the return losses of less than 25 dB have similar tendency. When $\Gamma_{Txa}\Gamma_{Rxa}I^2$ is comparable to $(\Gamma_{Txa} + \Gamma_{Rxa})I_a TI$ in equation (10), the phases of the reflection coefficients have a significant effect on the Tx leakage level. The local minimum of the Tx leakage map in Figure 7(a) appears when $\Gamma_{Txa}\Gamma_{Rxa}I^2$ and $(\Gamma_{Txa} +$

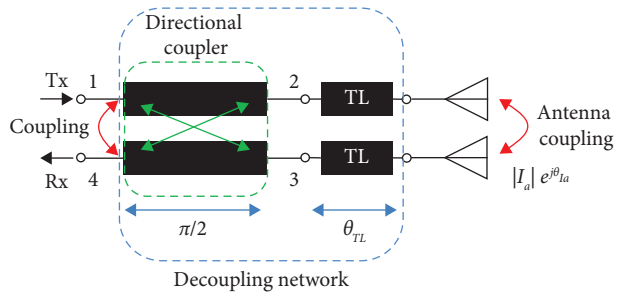

Figure 3: Schematic of Tx/Rx antennas with proposed decoupling network using single directional coupler and transmission lines.

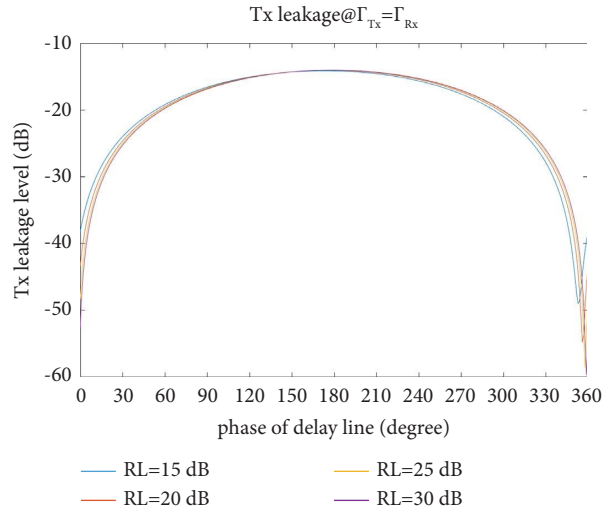

Figure 4: Tx leakage levels against the phase of the delay line from equation (7).

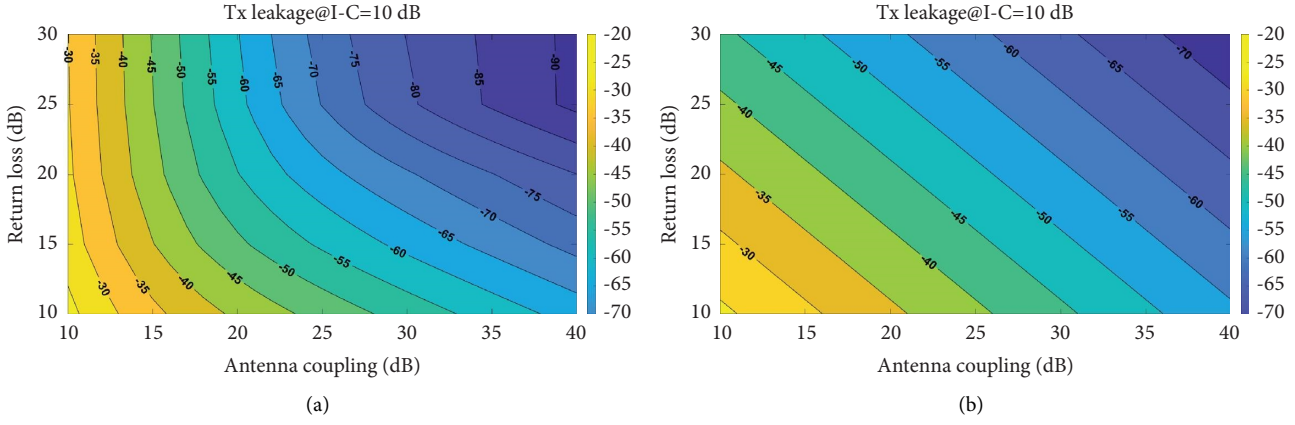

Figure 5: Tx leakage levels against the antenna coupling and return loss of the Tx and Rx antennas with $I - C = 10$ dB from (a) equation (7) and (b) equation (11).

$\Gamma_{Rxa})I_aTI$ have identical magnitudes but 180°-different phases. The Tx leakage level with the reflection coefficients of 10 dB in the proposed structure is less than −30.5 dB, which is better than the antenna without the decoupling network by 10.5 dB. The Tx leakage levels with the return losses of 15 and 20 dB against the phases of the reflection coefficients of the Tx and Rx antennas from equation (7) are depicted in Figures 8(a) and 8(b), respectively. The areas filled with yellow color for the return losses of 15 and 20 dB are corresponding to the Tx leakage

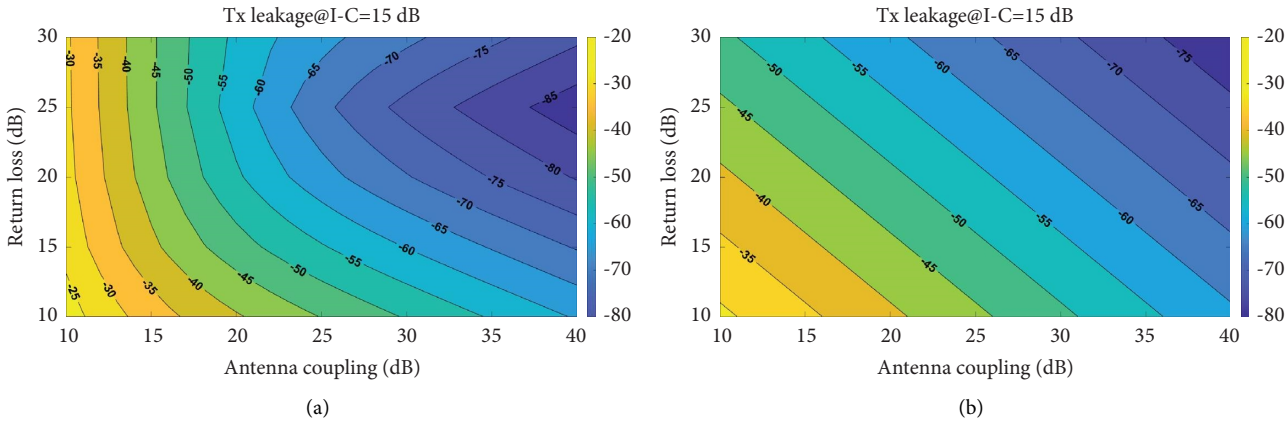

Figure 6: Tx leakage levels against the antenna coupling and return loss of the Tx and Rx antennas with $I - C = 15$ dB from (a) equation (7) and (b) equation (11).

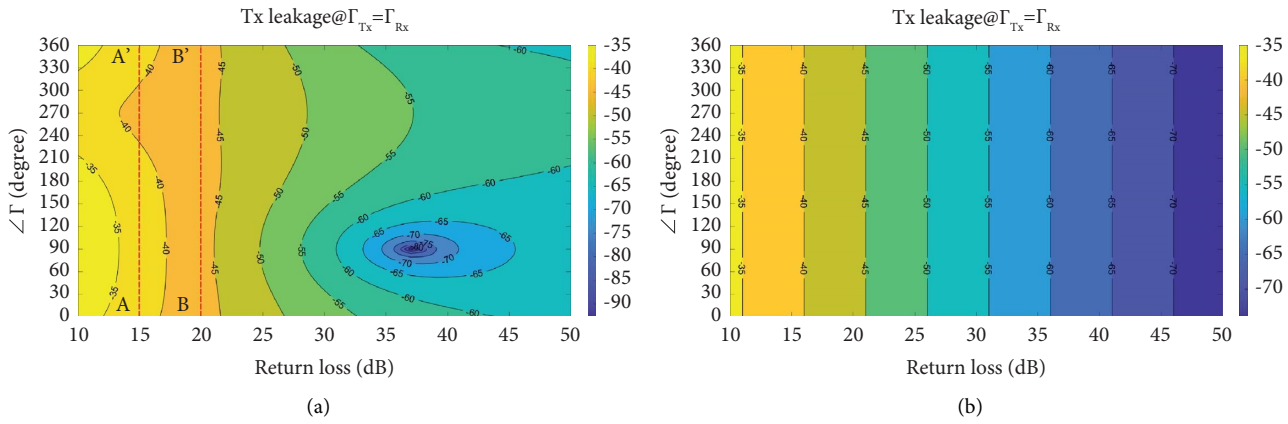

Figure 7: Tx leakage levels against the reflection coefficients of the Tx and Rx antennas with $\Gamma_{Txa} = \Gamma_{Rxa}$ from (a) equation (7) and (b) equation (11).

level of −38.9 and −43.8 dB, respectively, which are the worst cases. Consequently, as shown in Figures 7(a), 8(a), and 8(b), each Tx leakage level with the Tx/Rx antennas, of which the reflection coefficients are identical to each other, exhibits the worst Tx leakage levels, of which the magnitudes of the reflection coefficients are identical to each other (A-A′ and B-B′ in Figures 7(a), 8(a), and 8(b)). From the assumption of the antenna coupling with 20 dB, the Tx leakage level of less than −43.8 dB can be achieved by the proposed Tx leakage cancelation technique, providing that the return losses of Tx and Rx antennas are better than 20 dB. The influence of the antenna impedances on the Tx-Rx isolation is reduced by $\Gamma_a TC/\{(\Gamma_{Txa} + \Gamma_{Rxa})TI\}$ compared with the monostatic system adopting the directional coupler (Figure 1).

2.2. Design. By controlling the coupling factor of the directional coupler, C, to be equal to the magnitude of the antenna coupling, $|I_a|$ and the lengths of the transmission lines to meet the condition of $2\theta_{TL} + \theta_{Ia} = 2n\pi$, the Tx leakage signal in the Rx path (port 4 in Figure 3) is eliminated. Hence, the antenna coupling caused by space and surface waves can be canceled out by the coupling of the coupler as well as the transmission phases of both the lines.

To verify the proposed decoupling structure, two arrays of patch antennas, with each array consisting of four patch antennas in a 1×4 configuration, was designed for a K-band radar operation of 24 to 24.25 GHz, as shown in Figure 9, using the electromagnetic simulation software CST. It made use of the microwave substrate RO4350B with a thickness of 10 mil and a relative dielectric constant ε_r of 3.48. The dimensions of the antennas are listed in Table 1. The antennas were fed using 2.92 mm (K) connectors operating up to 40 GHz for measurement. The dimensions of the patch and the series-fed line were optimized to have resonance and high antenna gain at the center frequency and avoid beam tilting caused by the change in the progressive phase angle between adjacent elements along the series-fed line [26]. Also, series-fed lines were designed using meander lines to reduce the array size.

The S-parameters of the designed Tx/Rx antennas with distances of 2, 3, 5, and 9.5 mm, between elements, denoted as D in Figure 9, were extracted from simulation results using the software CST. The antennas with a distance 2 and

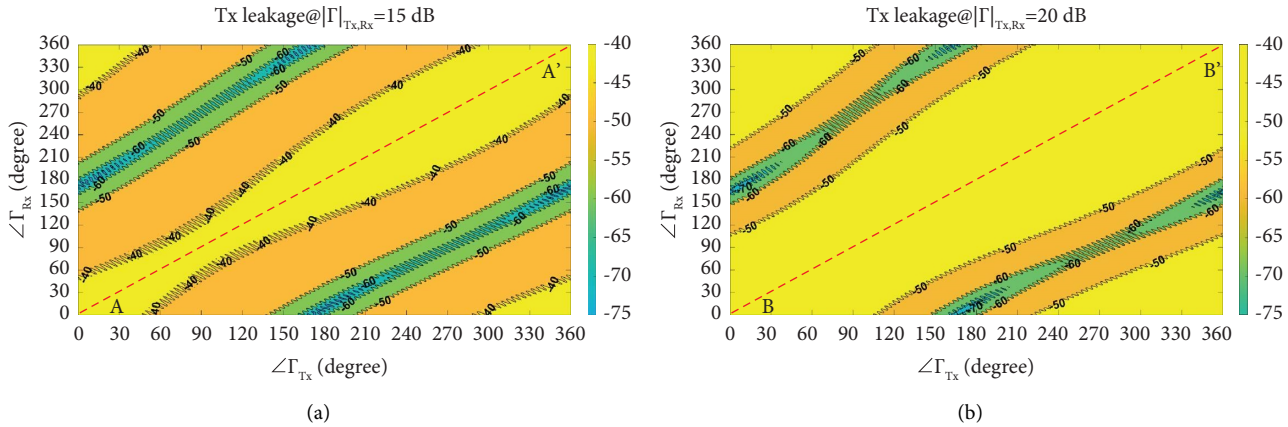

Figure 8: Tx leakage levels against the phases of the reflection coefficients of the Tx and Rx antennas with $\Gamma_{Txa,Rxa}$ = (a) 15 dB and (b)20 dB from equation (7).

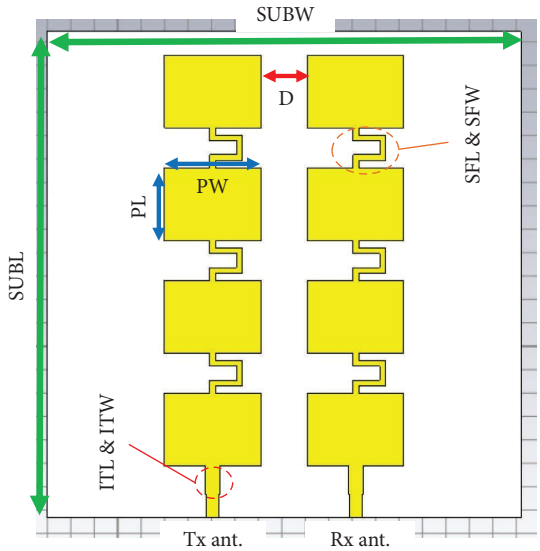

Figure 9: Geometry of Tx and Rx arrays.

Table 1: Dimensions of the array antenna.

Parameters	Descriptions	Values (mm)
PL	Length of the patch	3.12
PW	Width of the patch	4.1
ITL	Impedance transformer length	1.2
ITW	Impedance transformer width	0.64
SFL	Length of the series-fed line	4
SFW	Width of the series-fed line	0.25
D	Distance between elements	2
SUBL	Length of the substrate	20.74
SUBW	Width of the substrate	20.2
SUBH	Height of the substrate	0.254

3 mm including feed lines and decoupling networks were configured (Figure 3) and simulated using the software ADS. The antennas with a distance 5 and 9.5 mm including feed lines were also configured and simulated. In terms of the worst isolation at 24–24.25 GHz, the proposed Tx/Rx antennas including the decoupling network with a distance of 2 mm, showed a Tx/Rx isolation of 27.6–54.8 dB (minimum–maximum), which is comparable to Tx/Rx antennas without the decoupling network with a distance of 5 mm, having a Tx/Rx isolation of 27.8–29.0 dB. The proposed Tx/Rx antennas including the decoupling network with a distance of 3 mm provided a Tx/Rx isolation of 31.8–76.8 dB, which is comparable to Tx/Rx antennas without the decoupling network with a distance of 9.5 mm, showing a Tx/Rx isolation of 31.8–32.8 dB. For verification, a distance between array elements was set to 2 mm, corresponding 0.48 λ_0 between two adjacent arrays. The designed Tx and Rx antennas showed the magnitude and phase of the antenna coupling of 19.3 to 20.4 dB and −62.7° to −109.1°, respectively, at a range of 24 to 24.25 GHz, in simulation. Therefore, the coupling factor of the directional coupler and the electrical length of the added transmission line were determined as 20 dB and 138°, respectively, for optimal Tx leakage elimination at the operating frequency band.

Even-mode and odd-mode characteristic impedances of the designed directional coupler were set as 55.3 Ω and 45.2 Ω for 20 dB coupling coefficient. Figure 10 illustrates the Tx and Rx arrays using the proposed decoupling network with the sole directional coupler and transmission lines for controlling the magnitude and phase of the Tx leakages coupled by the directional coupler and the antennas, respectively. The antenna coupled Tx leakage is the vector sum of all Tx leakage paths denoted as Tx leakage flows 1, 2, 3, and 4 in Figure 10. The total Tx leakage signal that travels from green spot to Rx port in Figure 10, is the sum of both Tx leakages coupled by the directional coupler and the antennas. The total Tx leakage signal is suppressed since both signals have identical magnitudes and are out of phase.

The return losses of the Tx/Rx antennas without and with the decoupling network are shown in Figure 11. The Tx/Rx antennas without the decoupling network had 15-dB bandwidths (BWs) of 23.925–24.274 and 23.922–24.273 GHz, respectively, corresponding to fractional bandwidths (FBWs) of 1.45% and 1.46%. The Tx/Rx antennas with the

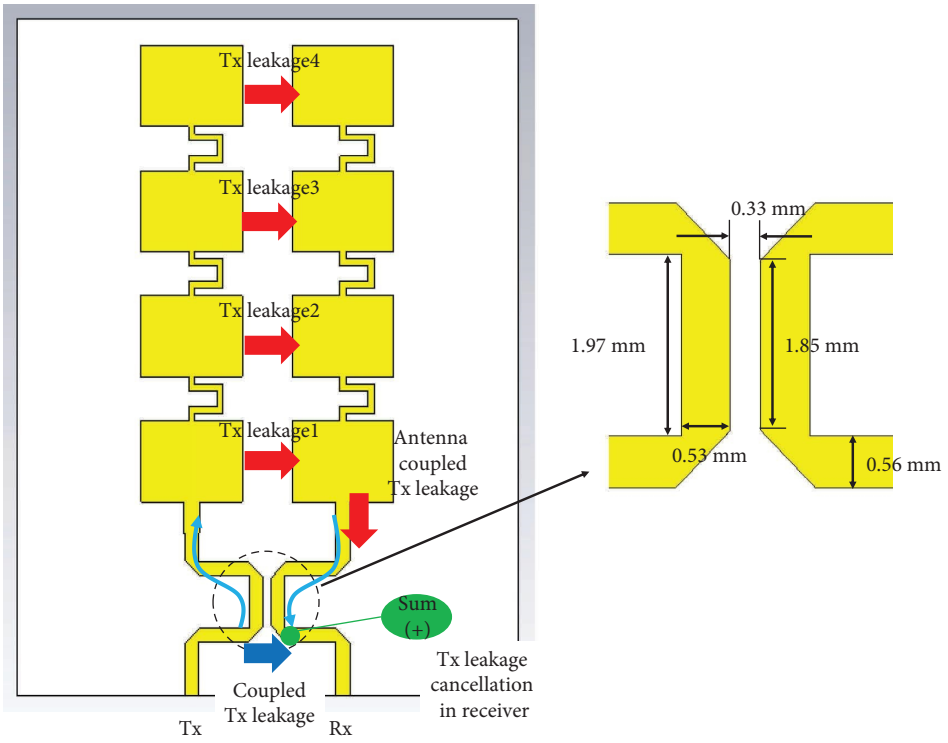

Figure 10: Tx and Rx arrays using the proposed decoupling network.

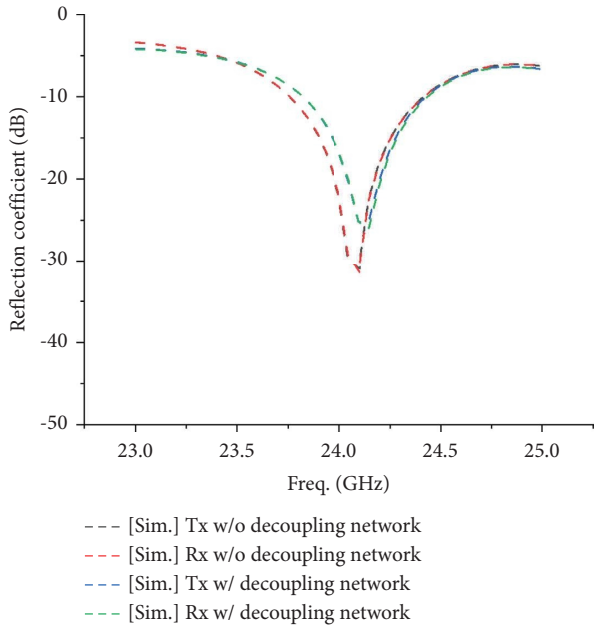

Figure 11: Reflection coefficients of the Tx/Rx antennas without and with the decoupling network.

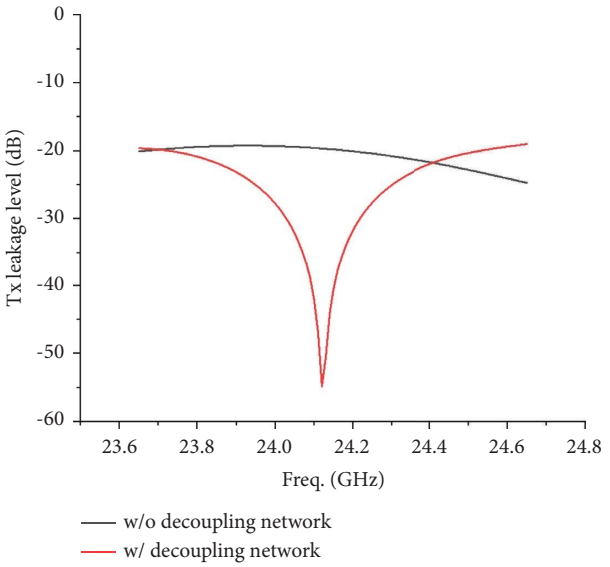

Figure 12: Tx leakage levels of the antennas without and with the decoupling network.

decoupling network provided 15-dB BWs (FBWs) of 23.962–24.238 GHz (1.15%) and 23.963–24.23 GHz (1.11%), respectively. The FBWs of the antennas with the decoupling network were slightly narrower than the antennas without the decoupling network. Figure 12 shows the simulated Tx leakage levels of the antennas without and with the decoupling network. The array antennas using the proposed decoupling structure showed a Tx-Rx isolation of 27.6–54.8 dB that had better performance at least by 7.2 dB compared with the conventional array antennas without the decoupling network. The BW of the Tx leakage cancelation is narrow due to the steep slope of the Tx-Rx isolation with −185.6°/GHz. The simulated beam patterns without and with the decoupling network at the frequency of 24.1 GHz for the

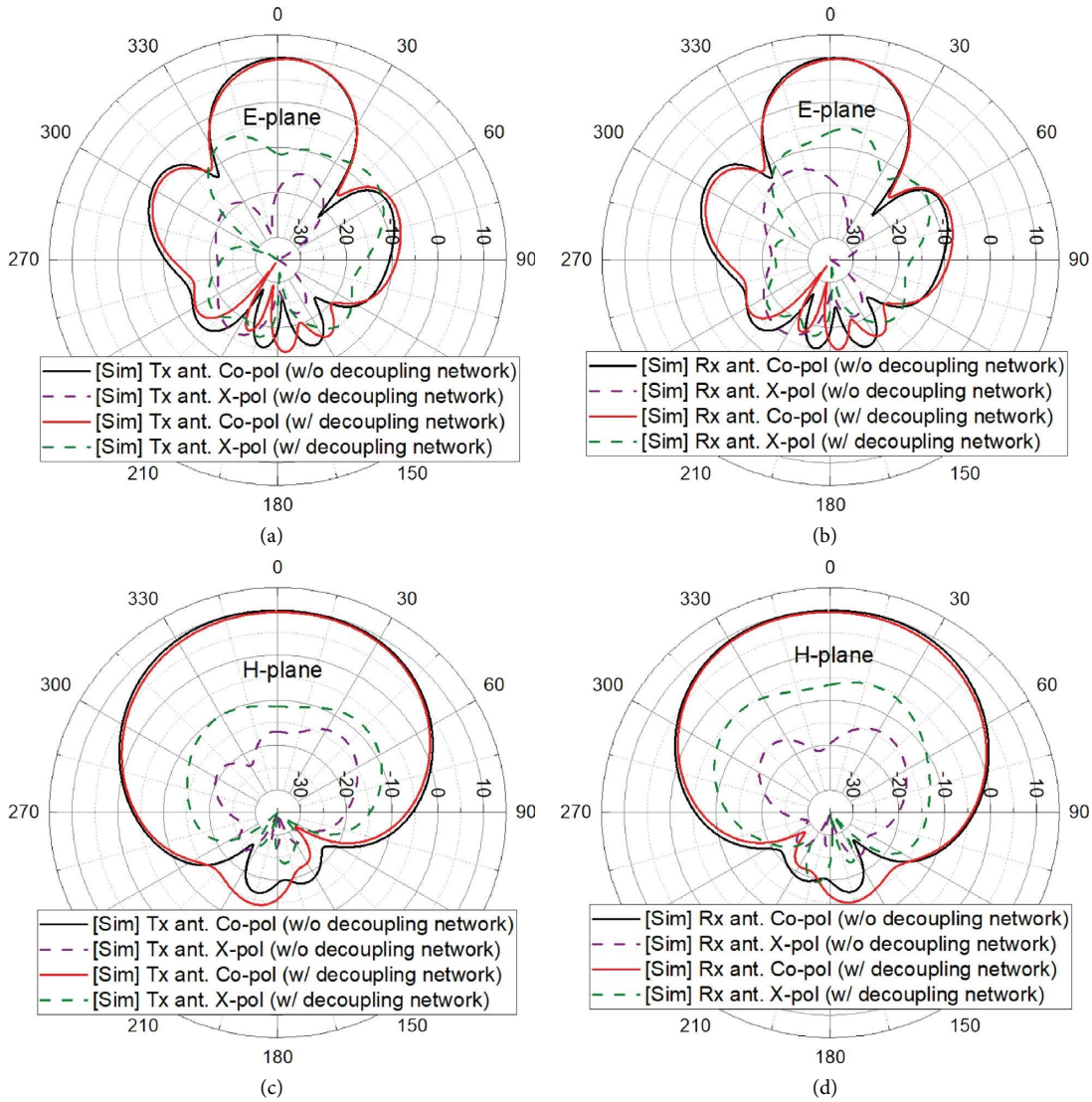

Figure 13: Simulated beam patterns of Tx/Rx antennas without and with the decoupling network at the frequency of 24.1 GHz: (a) E-plane of Tx antenna, (b) E-plane of Rx antenna, (c) H-plane of Tx antenna, and (d) H-plane of Rx antenna.

E-planes of the Tx and Rx antennas and H-planes of the Tx and Rx antennas are shown in Figures 13(a)–13(d), respectively. The Tx and Rx antennas without the decoupling network showed gains of 9.95 and 9.98 dBi, respectively. By comparison, the proposed antennas with the decoupling network provided gains of 9.64 and 9.75 dBi, respectively. The cross-polarized radiations of Tx and Rx antennas were increased by feed lines including the decoupling network (Figures 9 and 10). The simulated results in Figures 12 and 13 have proved that the decoupling network plays a key role in the enhancement of Tx leakage suppression with little variation in the Tx and Rx antennas beam patterns.

3. Experimental Verification

The construction procedure of the proposed Tx/Rx antennas with the decoupling network is as follows: First, Tx/Rx antennas without the decoupling network were designed and fabricated, and their isolations were measured. Next, the coupling coefficient of the directional coupler was chosen, being almost identical to the magnitude of the Tx/Rx antenna isolation, and the directional coupler was designed. Finally, the directional coupler and Tx/Rx antennas were connected by two transmission lines considering the phase of the Tx/Rx antenna isolation.

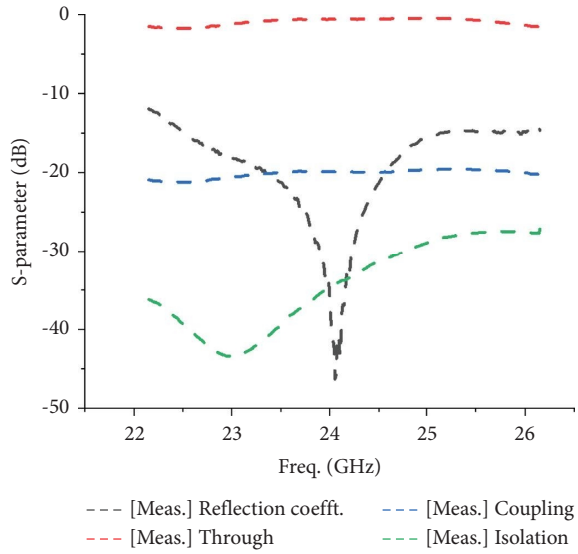

Figure 14: S-parameters of the fabricated 20 dB directional coupler.

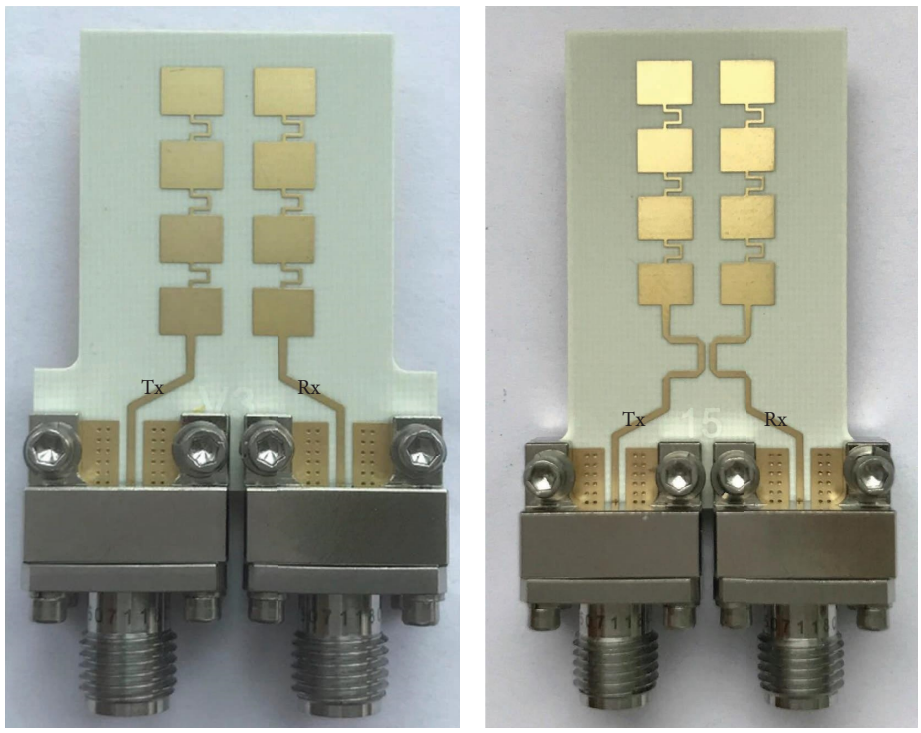

(a) (b)

Figure 15: Pictures of the Tx/Rx antennas (a) without and (b) with the decoupling network.

The directional coupler with 20 dB coupling coefficient was fabricated. The fabricated directional coupler showed a coupling coefficient of 19.7–20.1 dB and isolation of 32.8–33.5 dB at a range of 24–24.25 GHz as depicted in Figure 14. The 20 dB directional coupler and adjacently spaced Tx and Rx antennas were joined by two transmission lines with characteristic impedance of 50 Ω and electrical length of 138°. Figures 15(a) and 15(b) illustrate the pictures of the Tx/Rx antennas without and with the proposed decoupling network, respectively. The Tx/Rx antennas without the decoupling network had 15 dB BWs (FBWs) of 23.98–24.43 GHz (1.87%) and 23.98–24.50 GHz (2.16%), respectively. The Tx/Rx antennas with the decoupling network provided 15-dB BWs (FBWs) of 23.80–24.36 GHz (2.32%) and 23.80–24.45 GHz (2.69%), respectively. Each measured return loss of the proposed Tx/Rx antennas was

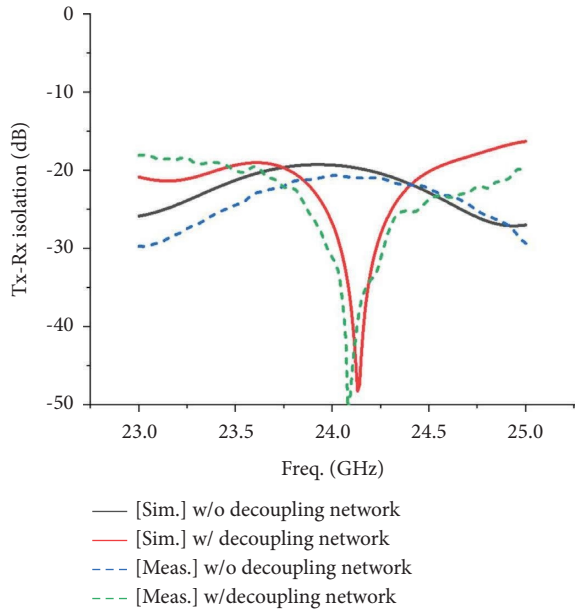

Figure 16: Tx to Rx isolations of the conventional Tx/Rx antennas without the decoupling network and the proposed ones with the decoupling network.

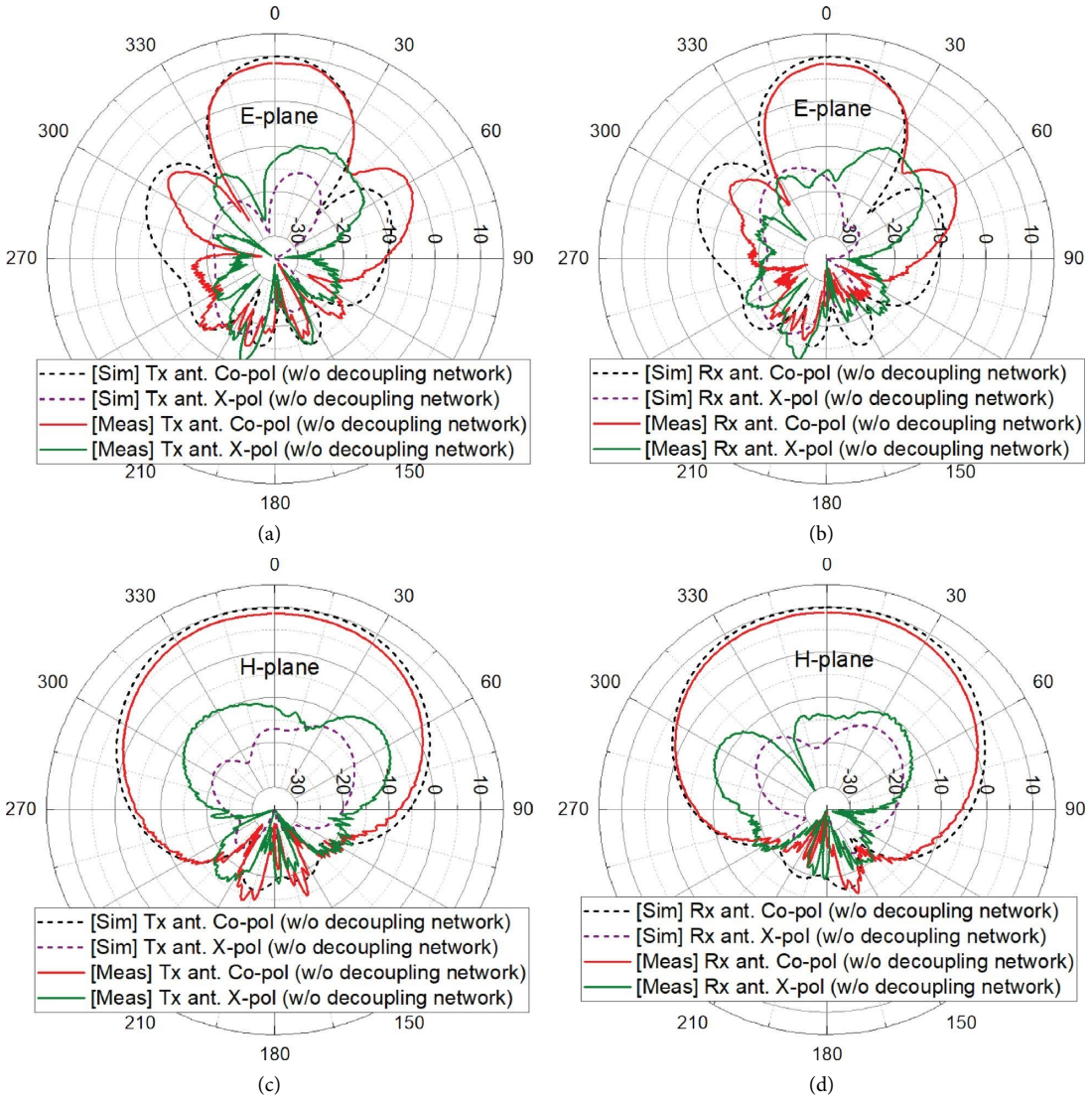

Figure 17: Measured beam patterns of Tx/Rx antennas without the decoupling network at the frequency of 24.1 GHz: (a) E-plane of Tx antenna, (b) E-plane of Rx antenna, (c) H-plane of Tx antenna, and (d) H-plane of Rx antenna.

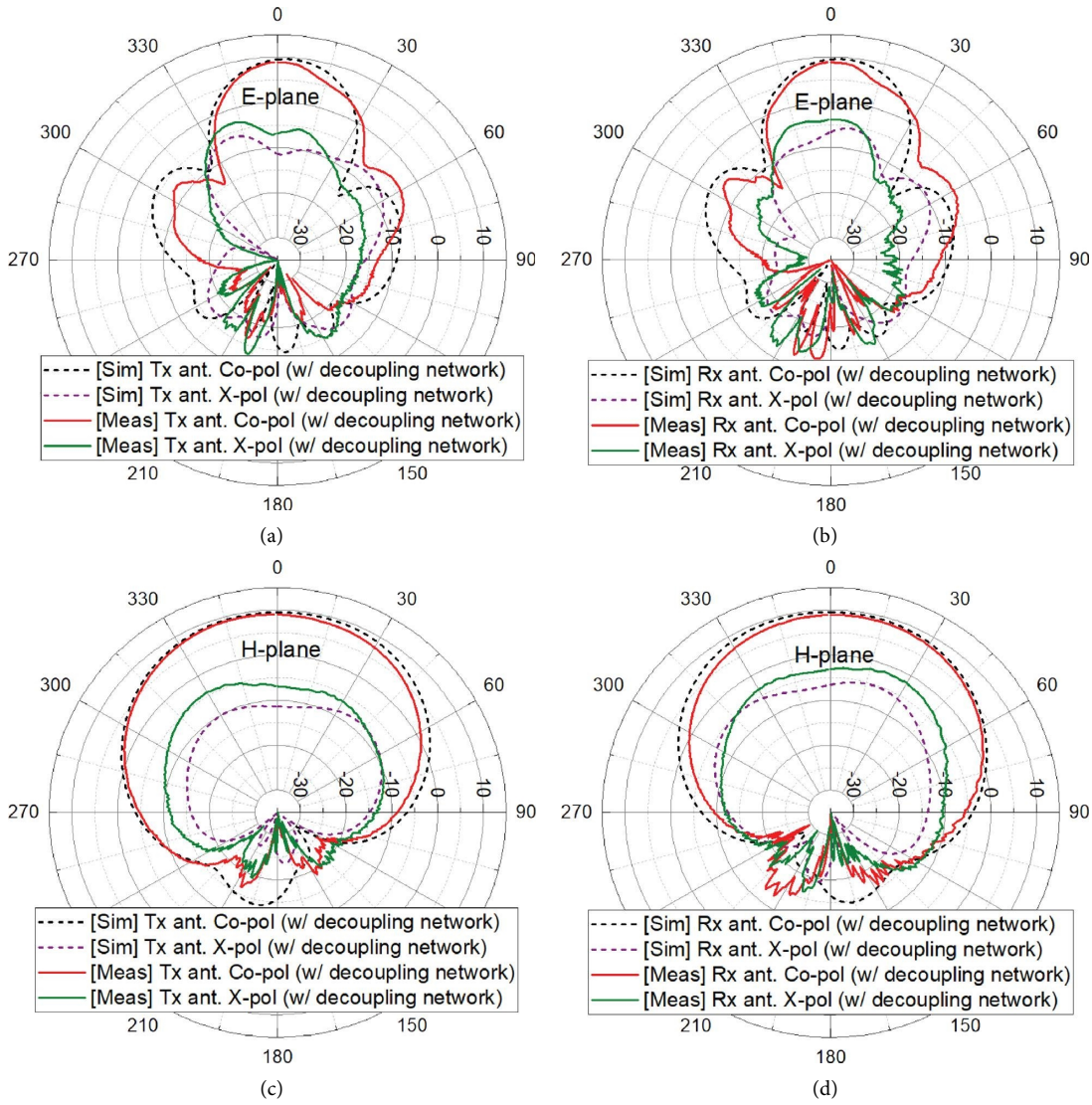

Figure 18: Measured beam patterns of Tx/Rx antennas with the decoupling network at the frequency of 24.1 GHz: (a) E-plane of Tx antenna, (b) E-plane of Rx antenna, (c) H-plane of Tx antenna, and (d) H-plane of Rx antenna.

above 20 dB at a range of 24–24.25 GHz. The measured isolations between Tx/Rx antennas without and with the decoupling network were 20.3–21.3 dB and 29.3–67.9 dB, respectively, at a range of 24–24.25 GHz, as shown in Figure 16. The proposed decoupling network results in better Tx-Rx isolation performance by more than 9 dB compared with the conventional Tx/Rx antennas without the decoupling network. For compacter size of the Tx/Rx antennas, ceramic directional couplers can be used instead of microstrip line directional couplers.

Figures 17(a)–17(d) and 18(a)–18(d) illustrate the measured beam patterns without and with the decoupling network at the frequency of 24.1 GHz, respectively. The proposed decoupling network had little effect on the beam patterns. The measured antenna gains of Tx and Rx without the decoupling network were 8.17 and 8.39 dBi at the frequency of 24.1 GHz, respectively. The measured antenna gains of Tx and Rx with the decoupling network were 8.72 and 8.73 dBi at the frequency of 24.1 GHz, respectively. The gains of the Tx/Rx antennas without and with the decoupling network were measured and the radiation efficiencies were calculated with the measured gains and simulated directivities. Figure 19 shows the measured gains and efficiencies of the Tx/Rx antennas without and with the decoupling network. The efficiencies of the Tx/Rx antennas without the decoupling network were 60.56% and 60.77% at the frequency of 24.1 GHz, respectively. The efficiencies of the Tx/Rx antennas with the decoupling network were 63.0% and 61.8% at the frequency of 24.1 GHz, respectively. The comparison between the proposed antenna and reported high isolation designs for monostatic, bistatic, and multiple-input multiple-output (MIMO) systems are listed in Table 2.

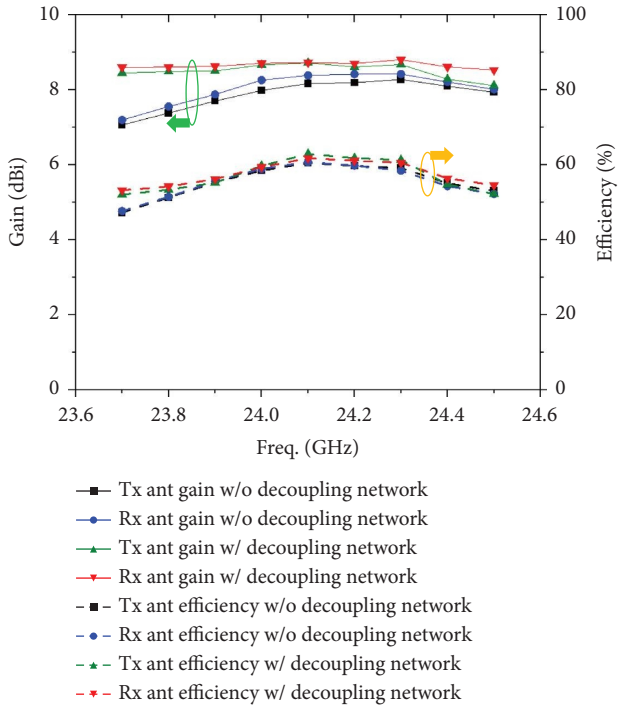

Figure 19: Measured gains and efficiencies of Tx/Rx antennas without and with the decoupling network.

Table 2: Comparison between the proposed antenna and reported high-isolation designs.

	Freq. (GHz)	Radiation element	Decoupling techniques	Gain (dBi)	Antenna size	Polarization	Tx-Rx isolation (dB)	The number of layers	Components	Notes
[5]	23.5–24.5	Dual fed 2 × 1 patch array	Orthogonal polarization, differential feed	6.97/ 5.65*	N.A	Dual-pol	>35	1	2 hybrid couplers, 2 quadrature couplers	Monostatic
[7]	22.7–24.8	2 × 1 patch array	Hybrid coupler	N.A	N.A	Co-pol	>30	1	5 hybrid couplers	Monostatic
[14]	7.5	Two patch	Two couplers connected by two sections of transmission line	6.88/ 6.55	$1.0\lambda_0\times 1.01\lambda_0\times 0.2125\lambda_0$	Co-pol	58	3	2 directional couplers	Bistatic
[15]	2.4–2.5	Two L-shaped antennas	Directional coupler, transmission line, resonant circuit, attenuator, phase shifter	N.A	$0.86\lambda_0\times 1.21\lambda_0$ (height N.A.)	Co-pol	>29	1	2 directional couplers, resonant circuit, 2 attenuators, phase shifter	Bistatic
[16]	2.45/5.25	Two dual-band monopole antennas	Reactive decoupling network using eigenmode feed network	2.3/ 0.7	$1.4\lambda_0\times 0.7\lambda_0\times 0.014\lambda_0$	Co-pol	30.3@ 2.45 GHz 34.3@ 5.25 GHz	1	2 reactive decoupling networks	MIMO
[17]	0.7–0.96	Two couple-fed PIFAs	Suspended transmission line with two terminals shorted to a ground plane and a capacitor	N.A	$0.22\lambda_0\times 0.42\lambda_0\times 0.0022\lambda_0$	Co-pol	>10@lower band, >15@upper band	1	Suspended transmission line	MIMO

Table 2: Continued.

	Freq. (GHz)	Radiation element	Decoupling techniques	Gain (dBi)	Antenna size	Polarization	Tx-Rx isolation (dB)	The number of layers	Components	Notes
[27]	13.6–15.7	4 × 4 patch	Orthogonal polarization, differential feed	22.4	$6.5\lambda_0\times 6.5\lambda_0\times 0.025\lambda_0$	Dual-pol	>50	1	—	Monostatic
[28]	27.6–29.5	LWA	Orthogonal polarization, differential feed	24	$11.7\lambda_0\times 11.7\lambda_0\times 0.3\lambda_0$	Dual-pol	>51	4	—	Monostatic
[29]	24–24.25	Two 2 × 2 patch	Electromagnetic bandgap	5.2/ 5.2*	N.A	Co-pol	>36.7 (>32@w/o decoupling)	1	Periodic Jerusalem cross slot array	Bistatic
This work	24–24.25	Two 1 × 4 patch	Directional coupler, transmission line	8.73/ 8.72*	$1.62\lambda_0\times 2.09\lambda_0\times 0.0204\lambda_0$	Co-HP	29.3–67.9 (>20.3–21.3@ w/o decoupling)	1	1 directional coupler	Bistatic

PIFA: planar inverted F antenna, LWA: leaky-wave antenna, HP: horizontal polarization, and *Tx/Rx.

4. Conclusion

This paper presents a new decoupling network using the sole directional coupler and transmission lines for closely spaced Tx/Rx antennas in radar applications with transmit and receive horizontal polarizations. The designed antenna structure has the advantages of good Tx-Rx isolation, compactness, Tx leakage insensitivity to the antenna impedance variation, and minute loss of Tx and Rx paths by virtue of the proposed decoupling network and the Tx and Rx antennas separation characteristic. The Tx-Rx isolation was improved by 9–47.6 dB due to the Tx leakage cancelation technique with the decoupling network, compared with the conventional Tx/Rx separated antennas. The suppressed Tx leakage is more insensitive to the antenna impedance variation compared with the conventional monostatic system using the quadrature hybrid, circulator, or directional coupler. The Tx and Rx paths have no loss excepting the line loss and coupler's though signal loss. Furthermore, the introduced decoupling network has little effect on beam patterns. Especially, the proposed decoupling structure can be easily applied to closely spaced Tx/Rx antennas in a compact radar module by adjusting the phase of the Tx leakage signal and the coupling coefficient of the directional coupler.

Data Availability

The data used to support the findings of this study are available upon request.

Conflicts of Interest

The authors declare that they have no conflicts of interest.

Acknowledgments

This work was supported by Institute of Information & communications Technology Planning & Evaluation (IITP) grant funded by the Korea Government (MSIT) (No. 2018-0-01658, Key Technologies Development for Next-Generation Satellites).

References

[1] H. H. Meinel, "Commercial applications of millimeter waves history, present status, and future trends," *IEEE Transactions on Microwave Theory and Techniques*, vol. 43, no. 7, pp. 1639–1653, 1995.

[2] M. Klotz and H. Rohling, "A 24 GHz short range radar network for automotive applications," in *Proceedings of the 2001 CIE International Conference on Radar Proceedings*, pp. 115–199, Beijing, China, October 2001.

[3] M. E. Russell, C. A. Drubin, A. S. Marinilli, W. G. Woodington, and M. J. Del Checcolo, "Integrated automotive sensors," *IEEE Transactions on Microwave Theory and Techniques*, vol. 50, no. 3, pp. 674–677, 2002.

[4] G. D. Martinson and M. M. Burin, "Radar detector technology," *Applied Microwave*, vol. 2, pp. 68–85, 1990.

[5] H. L. Lee, W.-G. Lim, K.-S. Oh, and J.-W. Yu, "24 GHz balanced Doppler radar front-end with Tx leakage canceller for antenna impedance variation and mutual coupling," *IEEE Transactions on Antennas and Propagation*, vol. 59, no. 12, pp. 4497–4504, 2011.

[6] J.-G. Kim, S. S. Ko, S. H. Jeon, J.-W. Park, and S. C. Hong, "Balanced topology to cancel Tx leakage in CW radar," *IEEE Microwave and Wireless Components Letters*, vol. 14, no. 9, pp. 443–445, 2004.

[7] C.-Y. Kim, J.-G. Kim, D. H. Baek, and S. C. Hong, "A circularly polarized balanced radar front-end with a single antenna for 24-GHz radar applications," *IEEE Transactions on Microwave Theory and Techniques*, vol. 57, no. 2, pp. 293–297, 2009.

[8] C.-Y. Kim, J.-G. Kim, and S. C. Hong, "A quadrature radar topology with Tx leakage canceller for 24-GHz radar applications," *IEEE Transactions on Microwave Theory and Techniques*, vol. 55, no. 7, pp. 1438–1444, 2007.

[9] T. H. Ho and S. J. Chung, "Design and measurement of a Doppler radar with new quadrature hybrid mixer for vehicle

applications," *IEEE Transactions on Microwave Theory and Techniques*, vol. 58, no. 1, pp. 1–8, 2010.

[10] M.-Q. Lee, "Lumped directional coupler with a varactor tuned reflector for RFID applications," *IEICE Electronics Express*, vol. 6, no. 2, pp. 129–134, 2009.

[11] H. L. Lee, D.-H. Park, and M.-Q. Lee, "A reconfigurable directional coupler using a variable impedance mismatch reflector for high isolation," *Journal of electromagnetic engineering and science*, vol. 16, no. 4, pp. 206–209, 2016.

[12] J. Li, S. Song, X. Chen, H. Nian, and W. Shi, "Design and implementation of a novel directional coupler for UHF RFID reader," *Electronics ETF*, vol. 20, no. 1, pp. 22–26, 2016.

[13] A. C. J. Malathi and D. Thiripurasundari, "Review on isolation techniques in MIMO antenna systems," *Indian Journal of Science and Technology*, vol. 9, no. 35, pp. 1–10, 2016.

[14] R. Xia, S. Qu, P. Li, Q. Jiang, and Z. Nie, "An efficient decoupling feeding network for microstrip antenna array," *IEEE Antennas and Wireless Propagation Letters*, vol. 14, pp. 871–874, 2015.

[15] H. Makimura, K. Nishimoto, T. Yanagi, T. Fukasawa, and H. Miyashita, "Novel decoupling concept for strongly coupled frequency-dependent antenna arrays," *IEEE Transactions on Antennas and Propagation*, vol. 65, no. 10, pp. 5147–5154, 2017.

[16] K.-C. Lin, C.-H. Wu, C.-H. Lai, and T. G. Ma, "Novel dual-band decoupling network for two-element closely spaced array using synthesized microstrip lines," *IEEE Transactions on Antennas and Propagation*, vol. 60, no. 11, pp. 5118–5128, 2012.

[17] W. Chen and H. Lin, "LTE700/WWAN MIMO Antenna System Integrated with Decoupling Structure for Isolation Improvement," in *Proceedings of the 2014 IEEE Antennas and Propagation Society International Symposium (APSURSI)*, pp. 689-690, Memphis, TN, USA, July 2014.

[18] S. Ghosh, T.-N. Tran, and T. Le-Ngoc, "Dual-layer EBG-based miniaturized multi-element antenna for MIMO systems," *IEEE Transactions on Antennas and Propagation*, vol. 62, no. 8, pp. 3985–3997, 2014.

[19] H. Qi, L. Liu, X. Yin, H. Zhao, and W. J. Kulesza, "Mutual coupling suppression between two closely spaced microstrip antennas with an asymmetrical coplanar strip wall," *IEEE Antennas and Wireless Propagation Letters*, vol. 15, pp. 191–194, 2016.

[20] C.-Y. Chiu, C.-H. Cheng, R. D. Murch, and C. R. Rowell, "Reduction of mutual coupling between closely-packed antenna elements," *IEEE Transactions on Antennas and Propagation*, vol. 55, no. 6, pp. 1732–1738, 2007.

[21] M. T. Islam and M. S. Alam, "Compact EBG structure for alleviating mutual coupling between patch antenna array elements," *Progress in Electromagnetics Research*, vol. 137, pp. 425–438, 2013.

[22] S.-W. Su, C.-T. Lee, and F.-S. Chang, "Printed MIMO-antenna system using neutralization-line technique for wireless USB-dongle applications," *IEEE Transactions on Antennas and Propagation*, vol. 60, no. 2, pp. 456–463, 2012.

[23] S. Zhang and G. F. Pedersen, "Mutual coupling reduction for UWB MIMO antennas with a wideband neutralization line," *IEEE Antennas and Wireless Propagation Letters*, vol. 15, pp. 166–169, 2016.

[24] C.-A. Yu, E. S. Li, H. Jin et al., "24 GHz horizontally polarized automotive antenna arrays with wide fan beam and high gain," *IEEE Transactions on Antennas and Propagation*, vol. 67, no. 2, pp. 892–904, 2019.

[25] V. V. Viikari, T. Varpula, and M. Kantanen, "Road-condition recognition using 24-GHz automotive radar," *IEEE Transactions on Intelligent Transportation Systems*, vol. 10, no. 4, pp. 639–648, 2009.

[26] F.-Y. Kuo and R.-B. Hwang, "High-isolation X-band marine radar antenna design," *IEEE Transactions on Antennas and Propagation*, vol. 62, no. 5, pp. 2331–2337, 2014.

[27] Y.-M. Zhang and J.-L. Li, "Differential-series-fed dual-polarized traveling-wave array for full-duplex applications," *IEEE Transactions on Antennas and Propagation*, vol. 68, no. 5, pp. 4097–4102, 2020.

[28] Q.-C. Ye, Y.-M. Zhang, J.-L. Li, G. F. Pedersen, and S. Zhang, "High-isolation dual-polarized leaky-wave antenna with fixed beam for full-duplex millimeter-wave applications," *IEEE Transactions on Antennas and Propagation*, vol. 69, no. 11, pp. 7202–7212, 2021.

[29] S. Kim, D. K. Kim, Y. Kim, J. Choi, and K. Y. Jung, "A 24 GHz ISM-band Doppler radar antenna with high isolation characteristic for moving target sensing applications," *IEEE Antennas and Wireless Propagation Letters*, vol. 18, no. 7, pp. 1532–1536, 2019.